

AD-A064 220

ROYAL AIRCRAFT ESTABLISHMENT FARNBOROUGH (ENGLAND)
THE EFFECT OF GRAIN STRUCTURE ON THE STRESS CORROSION RESISTANC--ETC(U)
APR 78 C J PEEL, P POOLE

F/G 11/6

UNCLASSIFIED

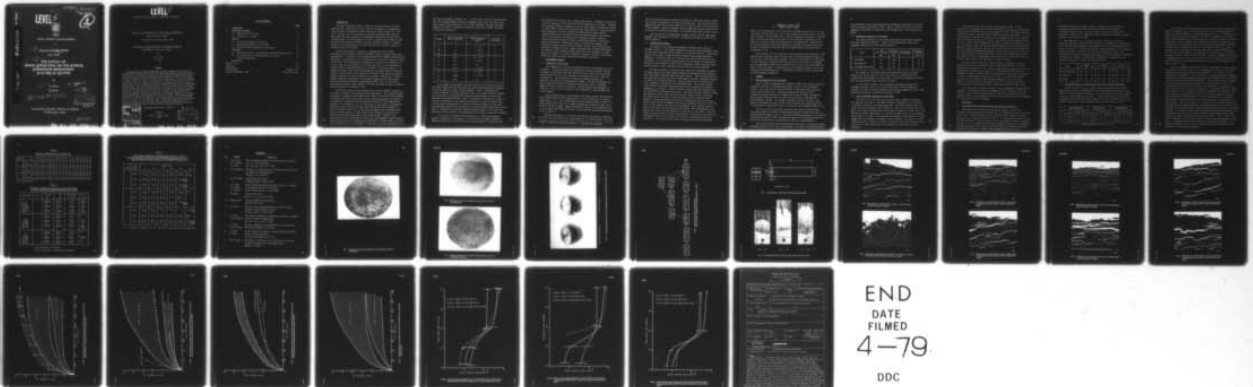
RAE-TR-78034

DRIC-BR-63423

NL

| OF |

AD
A064220



END
DATE
FILMED
4-79
DDC

TR 78034

ADA064220

FILE COPY

UNLIMITED

(18) DRIC

BR63423

(19)

TR 78034

LEVEL II



ROYAL AIRCRAFT ESTABLISHMENT

*

(9)

Technical Report, 78034

April 1978

(6)

**THE EFFECT OF
GRAIN STRUCTURE ON THE STRESS
CORROSION RESISTANCE
Al-Zn-Mg-Cu ALLOYS.**

by

(10)

C.J./Peel

P./Poole

(11)

Apr 78

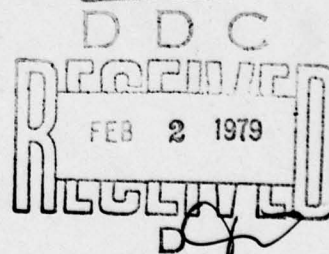
(12)

36p.

(14)

RAE-TR-78034

*



Procurement Executive, Ministry of Defence

Farnborough, Hants

310450

79 01 26 072

LEVEL II

UDC 669.715.5.721.3 : 669-17 : 620.194.2 : 669.018.8

ROYAL AIRCRAFT ESTABLISHMENT

Technical Report 78034

Received for printing 3 April 1978

THE EFFECT OF GRAIN STRUCTURE ON THE STRESS CORROSION RESISTANCE OF Al-Zn-Mg-Cu ALLOYS

by

C. J. Peel

P. Poole

SUMMARY

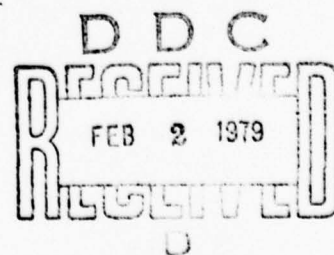
Three alloys, Al-6%Zn-2.5%Mg-1.5%Cu, Al-6%Zn-2.5%Mg-1.5%Cu-0.15%Zr and Al-6%Zn-2.5%Mg-1.5%Cu-0.17%Fe-0.15%Cr-0.11%Mn were produced as 37mm plate in the T6 condition. The stress corrosion resistance, fracture toughness and tensile properties of the alloys were determined to identify the effects of the grain refining elements, Zr, Cr, Fe and Mn on these properties. A special processing treatment, involving extensive precipitation and warm working, was also applied to pieces of plate to produce an extensively recrystallised structure, with a small grain size, for comparison with the coarser structures of the conventionally worked alloys. The results indicated that the alloy containing Fe, Cr and Mn had the highest stress corrosion resistance and strength but the lowest fracture toughness. The addition of 0.15% Zr to the quaternary alloy slightly improved the tensile strength and stress corrosion resistance but had no effect on fracture toughness. However this addition of Zr markedly improved the hot workability of the alloy and increased its tensile ductility. Special processing and working at 250°C was beneficial to the stress corrosion resistance of the quaternary alloy but detrimental to that of the other two alloys containing Zr or Fe, Cr and Mn. It was concluded that, in these Al-Zn-Mg-Cu alloys, a recrystallised grain structure has a low stress corrosion resistance and that inhibiting recrystallisation increases stress corrosion resistance.

Accession by	
BY	With Section <input checked="" type="checkbox"/>
DO	With Section <input type="checkbox"/>
UNANNOUNCED	<input type="checkbox"/>
JUSTIFICATION	
BY	
DISTRIBUTION/AVAILABILITY CODES	
Dist.	AVAIL. and/or SPECIAL
A	

Departmental Reference: Mat 344

Copyright

©
Controller HMSO, London
1978



79 01 26 072

LIST OF CONTENTS

	<u>Page</u>
1 INTRODUCTION	3
2 EXPERIMENTAL METHODS	5
2.1 Production of the alloys	5
2.2 Testing of the alloys	6
3 RESULTS	7
3.1 The microstructures of the alloys	7
3.2 Mechanical properties of the alloys	8
3.3 Stress corrosion resistance of the alloys	8
4 DISCUSSION	9
4.1 The interrelation of microstructure and mechanical properties	9
4.2 The interrelation of microstructure and stress corrosion resistance	10
5 CONCLUSIONS	12
Tables 1 to 3	14
References	16
Illustrations	Figures 1-26
Report documentation page	inside back cover

1 INTRODUCTION

The high strength Al-Zn-Mg-Cu alloys are used extensively in aircraft structures but, unfortunately, these alloys are susceptible to intergranular stress corrosion cracking particularly when aged to peak strength (T6). Day *et al*¹ reported that stress corrosion cracking of Al-Zn-Mg alloys occurred along high angle grain boundaries and Elkington² showed that the addition, to Al-Zn-Mg alloys, of certain elements such as Cr, promoted the formation of substructure and increased resistance to stress corrosion cracking. It appears, therefore, that susceptibility to stress corrosion may, at least in part, be controlled by grain structure.

During conventional hot working, at temperatures of about 450°C, Al-Zn-Mg-Cu alloys undergo a degree of dynamic recovery, recrystallisation and grain growth². The extent of this dynamic behaviour will depend on the amount of deformation, the temperature of hot working and the inclusion or particle content of the alloy. The total amount of deformation is limited by the dimensions of the cast ingot and the thickness of the final plate and, in the production of aircraft plate, a 300%-600% reduction in thickness by rolling is normal⁴. In commercial practice cast ingots are produced as rectangular slabs and these are rolled in the direction of the long axis of the slab. This type of production sequence could not be fully reproduced in the present research and, in order to achieve sufficient deformation, the cylindrical ingots were initially upset pressed reducing their height by approximately 200%. This was followed by pressing and rolling at right angles to the first operation in order to achieve a further reduction in thickness of 350%.

The particle content of the as-worked alloy has an important influence on the degree of dynamic recrystallisation and grain growth. The recrystallisation temperature of commercial Al-Zn-Mg-Cu alloys tends to be reduced by the presence of elements which are totally soluble at the working temperature but raised by the presence of elements which are relatively insoluble at this temperature⁵. Elements of low solubility, *eg* Fe, are present in the alloys as intermetallic particles even in the cast structure, while the distribution of elements of greater solubility such as Si, or even Mg, will depend upon the working treatments and diffusivities. To some extent the distribution of particles will depend upon the partitioning that occurs during casting. Elements, with equilibrium partition coefficients of less than unity segregate towards dendrite arm boundaries and if the solubility and diffusivity of these elements is low the initial dendrite size will determine, to some extent, the final distribution of

particles and possibly the grain size. It can be seen, from the following table, that the alloying elements, added to Al-Zn-Mg-Cu alloys, fall into three basic types; those of high solubility (>1% at 500°C) frequently with associated high diffusivity, those of intermediate solubility (0.2%-1.0% at 500°C), and those with very low solubility.

Element	Solid solubility in pure Al at 500°C %	Diffusivity in pure Al at 500°C m^2s^{-1}	Partition coefficient
Cu	4	4×10^{-14}	<1
Mg	12	4×10^{-13}	<1
Zn	>40	9×10^{-13}	<1
Mn	0.35	1.5×10^{-13}	>1
Si	0.8	1×10^{-13}	<1
Ti	0.2	na	>1
V	0.37	1.7×10^{-17}	>1
Cr	0.15	5×10^{-16}	>1
Fe	0.006	5×10^{-16}	<1
Zr	0.05	na	>1

In the present investigation the grain structure of three alloys based on Al-6.0%Zn-2.5%Mg-1.5%Cu has been varied by special thermo-mechanical treatments and by the addition of grain refining elements. Alloy 1, containing only 5.6% Zn, 2.5% Mg and 1.5% Cu, was expected to have a low recrystallisation temperature resulting in recrystallisation and grain growth during conventional hot pressing and rolling operations. Alloy 2, containing an addition of 0.15%Zr, is similar in composition to the commercial alloy 7010. It was anticipated that, for this alloy, conventional hot working at 450°C would result in a partially recrystallised microstructure and that the Zr addition would inhibit grain growth. Alloy 3 containing Fe, Cr and Mn, elements normally present in 7075 alloy, was expected to have a partially recrystallised structure after conventional treatment.

In an attempt to promote recrystallisation, but inhibit grain growth, special processing was also employed. In this process an ageing treatment at 380°C was carried out, after the first hot pressing stages, to precipitate all

the available Zn, Mg and Cu and to inhibit grain growth. Subsequent conventional solution treatment at 465°C will take these precipitates into solution. Moreover, after ageing at 380°C , the temperature of the final stages of working was reduced to either 300°C or 250°C , thus increasing the stored energy for recrystallisation during subsequent solution treatment and inhibiting the normal dynamic recrystallisation that would have occurred during conventional hot working at 450°C . This special processing was thus designed to produce a heavily recrystallised microstructure of small recrystallised grains in which grain growth was inhibited. These special grain structures were compared with conventional microstructures in which dynamic recovery and recrystallisation resulted in elongated 'as cast' grains containing small recrystallised grains. The effects of these changes in grain structure on the resistance to stress corrosion cracking, in the short transverse direction, have been investigated using both C-ring and double cantilever beam (DCB) test pieces.

2 EXPERIMENTAL METHODS

2.1 Production of the alloys

The compositions of the three alloys selected for investigation are given in Table 1. Cylindrical ingots were prepared by a modified Durville casting technique in which the molten alloy was poured into a thin walled steel mould. Once the mould was full, water was fed at a controlled rate into a tank that surrounded it. This resulted in a moving solid-liquid interface that travelled up the mould at approximately 75 mm/min. The melt was degassed and grain refined shortly before pouring with proprietary tablets containing hexachlor-ethane and boron tri-chloride. The cast ingots were homogenised at 450°C for 16 hours and then scalped to final dimensions of 330 mm length and 115 mm diameter.

Etched macro-sections of the bottoms of the ingots revealed the beneficial grain refining effects of the additions of Zr or Cr, Fe and Mn at the casting stage (Figs 1 to 3). The scalped ingots were hot pressed (450°C or 400°C) to a cheese shaped billet (Fig 4) in a single pressing that reduced the ingot from 330 mm to 150 mm in height. Again the beneficial effects of the additions of Zr or Cr, Mn and Fe were apparent (Fig 4), in particular the grain refining effects of the Zr addition.

The three cheeses were cut in half, one half was hot pressed transversely at 450°C * and then rolled at the same temperature to 37 mm thickness. The other

* 400°C , in the case of high purity Alloy 1, to prevent hot shortness

half of the billet was heat treated for 100 hours at 380°C and pressed at 300°C , in a direction transverse to the axis of the cast ingot. This piece was halved again and one half was rolled at 300°C and the other at 250°C to produce plate of 37 mm thickness. This heat treatment and low temperature working procedure will be referred to as special processing. A processing flow chart is shown in Fig 5.

All the plates were solution heat treated at $465^{\circ}\text{C} \pm 2^{\circ}\text{C}$ for three hours, quenched into cold water at $18^{\circ}\text{C} \pm 2^{\circ}\text{C}$, and aged for 26 hours at $121^{\circ}\text{C} \pm 1^{\circ}\text{C}$ to the T6 condition.

2.2 Testing of the alloys

The results of the conventional mechanical testing of the alloys are included in Table 2. The tensile properties of each alloy were determined using two test pieces machined from the plates in a transverse direction. Short transverse stress corrosion properties were determined using C-rings alternately immersed in 3.5% NaCl solution for 10 minutes and dried in laboratory air for 50 minutes. Every C-ring was microsectioned in the mid-plane, on completion of testing, and was examined at times 500 for evidence of stress corrosion cracks. Further details of this conventional test method can be found elsewhere⁶.

The rates of growth of stress corrosion cracks were determined for each of the three alloys in the three conditions using the decreasing stress intensity test⁷ with double cantilever beam test pieces (Fig 6). Two test pieces were cut from each piece of plate so that the cracks grew in the short transverse plane of the plates in the rolling direction. The test pieces were all loaded until a crack 'popped-in' from the root of the machined notch. The stress intensity factor at which this pop-in occurred was noted and is quoted as the fracture toughness K_{Ic} , in Table 2. Neutral 3.5% NaCl solution was then introduced into the notches of the pre-loaded test pieces. The growth of stress corrosion cracks was monitored on both sides of the test pieces, using an optical travelling microscope, and in the centre of the test pieces using an ultrasonic crack detector. The test solution was fed into the cracks twice daily and the test pieces stood vertically throughout the test in a humidified cabinet at $20^{\circ}\text{C} \pm 1^{\circ}\text{C}$. Plots of crack growth, from the tip of the popped-in crack, against time were made for each test piece (eg Fig 20) and from these curves instantaneous crack growth rates (da/dt) could be measured as a function of crack depth. Since the crack tip stress intensity factor is also known as a function of crack depth, the crack growth rates could be plotted as a function of stress intensity factor (eg Fig 24). The stress intensity factor was calculated from the expression

$$K_1 = \frac{\delta v E h [3h(a + 0.6h)^2 + h^3]^{\frac{1}{2}}}{4[(a + 0.6h)^3 + h^2 a]}$$

where δv is the deflection at the load-line on loading to pop-in, and a is the crack depth from the load-line. $2h$ is the thickness of the test piece. The load-line was taken to be the centre line of the two opposing bolts (Fig 6). A further minor correction was made for the effect of the reduction in thickness of the beams at the notches, this correction need not be detailed here. Solutions for the stress intensity factor were computed and tabulated for deflections of up to 0.5 mm, in increments of 0.01 mm, and crack lengths between 8 mm and 50 mm in increments of 1 mm.

After testing, for up to 2000 hours, the test pieces were broken open. The exposed crack fronts were clearly curved (Fig 7) demonstrating the necessity for the ultrasonic crack detection technique. An error in measurement of crack depth of 5 mm is possible with such curved crack fronts and will result in a maximum error of approximately 30% in the calculated value of K at 15 mm crack depth and 20% at 30 mm crack depth. This potential error outweighs any other, such as the accuracy of the measurement of δv . The broken test pieces were micro-sectioned for metallographic examination.

3 RESULTS

3.1 The microstructures of the alloys

Alloy 1, given a conventional hot working at 400°C, had a fully recrystallised grain structure of large equi-axed grains at least 0.1 mm in diameter (Fig 8). The cracks seen in the micro-section are secondary stress corrosion cracks below the main crack. Special processing with rolling at 300°C considerably reduced the amount of dynamic grain growth so that, although the grain structure was equi-axed, the grain size was halved to approximately 0.05 mm diameter (Fig 9). In contrast, the grain structure of alloy 1, when specially processed and rolled at 250°C, was only partially recrystallised and the recrystallised grains were found to be only 0.01 mm in diameter (Figs 10, 11).

Alloy 2, in each of the three conditions, had a partly recrystallised structure although, as intended, special processing had increased the extent of recrystallisation (Figs 12 to 15). Reducing the working temperature of the special processing from 300°C to 250°C increased the number of recrystallised grains but reduced the average size of these grains by a factor of approximately 2.

Alloy 3 was also partially recrystallised after each of the three processing treatments (Figs 16 to 19) and, as with alloy 2, the extent of recrystallisation

was increased by special processing and by reducing the temperature of the final rolling treatment from 300°C to 250°C. Again, a reduction in the final rolling temperature from 300°C to 250°C reduced the average size of the recrystallised grains.

3.2 Mechanical properties of the alloys

The tensile properties of the three alloys showed several general trends with alloy composition (Table 2). These are illustrated below, where mean mechanical properties have been taken from Table 2.

Alloy	0.2% Proof strength MPa	Tensile strength MPa	Elongation % (on 5.6√A)	Fracture toughness MPa m ^{1/2}
1 Al-Zn-Mg-Cu	461	526	6	27
2 Al-Zn-Mg-Cu-Zr	474	542	15	28
3 Al-Zn-Mg-Cu-Fe-Cr-Mn	490	564	12	23

The strength of the alloys clearly increases with the extra alloying additions but the ductility of alloy 2 was excellent, consistent with the exceptionally good formability of this alloy. The fracture toughness of alloys 1 and 2 was considerably better than that of alloy 3.

It can be seen in Table 2 that the special processing increased the strengths of alloys 2 and 3, with little effect upon fracture toughness or ductility, but that the tensile properties and fracture toughness of alloy 1 were reduced by the special processing and working at 250°C.

3.3 Stress corrosion resistance of the alloys

The results of the C-ring stress corrosion tests, summarised in Table 3, were somewhat inconclusive. The stress corrosion resistance of all the alloys, in the three conditions, was surprisingly high. The results indicate that the stress corrosion threshold stress for alloy 1, in any of the three working treatments, was at least 250 MPa, whilst the threshold stresses for alloys 2 and 3 were 200 MPa and 250 MPa respectively. In contrast, previous tests of an Al-Zn-Mg-Cu alloy identical to alloy 1 in composition, but produced as plate without an upset forging step, had revealed a threshold stress of 185 MPa. The reasons for these differences are not understood. However, the present work does indicate that the addition of Zr grain refiner may not be beneficial to the stress corrosion resistance.

The results of the stress corrosion crack growth studies were more conclusive. A comparison of the crack extension-test time data for the different alloys (Figs 20 to 22) shows that the crack growth in alloy 2 was consistently more rapid than in alloy 3, whichever alloy production route is considered. This comparison should be treated with caution since, although the pop-in crack lengths were very similar for all the test pieces, the starting stress intensity factors for alloy 2 were slightly higher than for alloy 3, because of the higher K_{Ic} of alloy 2. However, since the special processing appeared to have had no significant effect upon crack growth rates in either alloy 2 or alloy 3, the results for the three processing methods are combined in Fig 23 and it can be seen that, for all these results, the crack growth rates in alloy 2 were significantly higher than those in alloy 3. Surprisingly, the cracks in alloy 3 could take up to ten times as long to grow to the same depth as cracks in alloy 2.

If the crack growth data, for alloys 2 and 3, is compared on a stress intensity factor basis a consistent trend is again observed for each of the production routes (Figs 24 to 26). Thus, at high stress intensity factors the Zr bearing alloy 2 appears better than alloy 3, reflecting the higher fracture toughness of alloy 2, whilst at lower stress intensity factors, the crack growth in alloy 3 is significantly slower than in alloy 2, in accord with previous statements on the relative stress corrosion resistance of the two alloys. Figs 24 to 26 show the mean crack growth curves for each alloy and condition, with error bars to represent the width of the scatter bands for these tests.

The results for the high purity alloy 1 show a dependence upon the working procedure. The crack growth rates in samples of alloy 1, worked at 400°C and 300°C, were very rapid but after working at 250°C the crack growth rates were markedly reduced. This improvement in stress corrosion resistance was accompanied by a reduction in fracture toughness.

4 DISCUSSION

4.1 The interrelation of microstructure and mechanical properties

The tensile test results indicated that the addition of Zr to the Al-Zn-Mg-Cu alloy significantly increased both the strength and tensile ductility of the alloy. These improvements must be associated with the grain refining effects of $ZrAl_3$ particles present in alloy 2. A similar grain refinement, with the addition of Fe, Cr and Mn, produced an even more marked increase in strength for alloy 3. It is thought that the further strength increase must be associated with the introduction of relatively large quantities of intermetallic particles containing Fe, Cr and Mn. However, these intermetallic particles had a

detrimental effect upon fracture toughness, consistent with the results of previous research⁸ on the effects of Fe upon the fracture toughness of Al-Zn-Mg-Cu forging alloys. The lower volume fraction of very small $ZrAl_3$ particles in alloy 2 had no significant effect upon fracture toughness, again in agreement with previous findings⁹.

There appeared to be a consistent trend for each alloy in which the strength of the alloy increased with an increase in the extent of recrystallisation. Thus the special processing was beneficial to the strength properties of alloys 2 and 3, as it increased the extent of recrystallisation, yet detrimental to those of alloy 1. The marked reduction in properties for alloy 1 was associated with special processing and rolling at 250°C which produced a partially recrystallised structure. Average tensile properties are summarised in the following table with the extent of recrystallisation.

Alloy	Alloy 1			Alloy 2			Alloy 3		
	400	300	250	450	300	250	450	300	250
% Recrystallised	100	100	75	30	60	60	10	50	80
0.2%PS, MPa	466	470	448	463	478	483	485	493	494
TS, MPa	534	534	512	529	544	553	550	569	574

4.2 The interrelation of microstructure and stress corrosion resistance

Average values for K_{Isc} are shown below and are compared with a semi-quantitative indication of the extent of recrystallisation of the three alloys after the three processing treatments. K_{Isc} was defined as the stress intensity factor at a crack growth rate of $1 \mu m h^{-1}$. The microstructural data was taken from samples of both DCB test pieces used for each alloy condition and relevant figures, illustrating typical microstructures, are indicated in the table.

Alloy	Conventional processing rolling at 400°C or 450°C			Special processing rolling at 300°C			Special processing rolling at 250°C		
	% Recrystallised	Grain size mm	K_{Isc} MPa m ^{1/2}	% Recrystallised	Grain size mm	K_{Isc} MPa m ^{1/2}	% Recrystallised	Grain size mm	K_{Isc} MPa m ^{1/2}
1	100 (Fig 8)	0.1	7.5	100 (Fig 9)	0.05	4*	75 (Fig 10)	0.01	12
2	30 (Fig 12)	0.01	10.5	60 (Fig 14)	0.05	7.5	60 (Fig 15)	0.01	7
3	10 (Fig 16)	0.005	13	50 (Fig 17)	0.02	16	80 (Fig 18)	0.01	10

* Cracks did not grow down the centres of the test pieces

It is evident from the above table that there is no consistent correlation between the values of K_{lsc} and the average size of the recrystallised grains. However, there does appear to be a general tendency for K_{lsc} to decrease as the extent of recrystallisation increases. This trend is apparent in the case of alloy 1 where specimens with fully recrystallised structures exhibited relatively rapid rates of stress corrosion crack growth and relatively low values of K_{lsc} compared with the corresponding data for the partially recrystallised material. A similar trend is evident for alloy 2, *ie* the lowest values of K_{lsc} were obtained for the specimens with the most extensively recrystallised structures. One exception to this trend is illustrated by the values of K_{lsc} obtained for specimens of alloy 3 worked at 450°C and 300°C. However, it should be noted that, in agreement with the results for alloys 1 and 2, the specimens of alloy 3 with the most extensively recrystallised structures (worked at 250°C) exhibited the lowest values of K_{lsc} .

It has been suggested previously¹⁰ that the improvement in stress corrosion resistance of Al-Zn-Mg-Cu alloys with T73 ageing may be associated with the redistribution of solute atoms near grain boundaries. It is possible that the apparently low resistance to stress corrosion of recrystallised grain boundaries, compared with unrecrystallised boundaries, may also be associated with variations in solute distribution near grain boundaries. The distribution of Cu is thought to be of particular importance although, in the case of alloys 2 and 3, the distribution of Zr, Mn, Fe and Cr must also be considered. In addition to any electrochemical effects caused by the presence of intermetallic particles containing Zr, Mn, Fe or Cr, it should be noted that intermetallic particles can affect the nucleation of the precipitation of the main hardening phase $Mg(Zn_xCu_yAl_y)$ thereby producing further changes in the local distribution of Zn, Mg and Cu. The presence of intermetallic particles affects precipitate nucleation in two similar ways. Firstly, differences in the coefficients of thermal expansion for the particles and the matrix generate stresses on quenching and can result in the production of dislocation loops. These dislocations readily nucleate precipitation. Secondly, the presence of these particles promotes substructure and partially recrystallised structures and the large increase in grain boundary length again markedly increases heterogeneous precipitate nucleation. Thus, in effect, the alloys containing Zr, Cr, Mn and Fe should be more extensively precipitated than alloy 1, although the three alloys received the same ageing treatment. It is generally accepted that the stress corrosion resistance of Al-Zn-Mg-Cu alloys increases with over-ageing treatments.

In agreement with the stress corrosion resistance data obtained with C-ring specimens the crack growth studies indicate that, for each production route, alloy 3, containing Fe, Mn and Cr, had lower crack growth rates and higher values of K_{Isc} than alloy 2, which contained Zr. The lowest resistance to stress corrosion was observed for those specimens of alloy 1 which had fully recrystallised structures. The results for alloys 1 and 3 are in agreement with the work of Hinton¹¹, who reported that the addition of 0.2%Cr to Al-5.7%Zn-2.7%Mg-1.3%Cu alloy, aged for 24 hours at 121°C, reduced the rate of crack growth and increased K_{Isc} (K where crack velocity was $1 \mu\text{m h}^{-1}$) from $14.5 \text{ MPa m}^{\frac{1}{2}}$ to $17 \text{ MPa m}^{\frac{1}{2}}$. However, the reasons for this effect were not discussed and the effect of the Cr addition on microstructure was not reported.

It appears that several factors may be responsible for the variations in stress corrosion resistance of alloys 1, 2 and 3. The inhibition of recrystallisation by the addition of Zr or Cr, Fe and Mn appears to be beneficial, but detailed considerations of solute distribution near grain boundaries may be necessary to explain the superior properties of alloy 3, containing Cr, Fe and Mn.

5 CONCLUSIONS

- (1) The addition of 0.17% Fe, 0.15% Cr and 0.11% Mn to Al-6%Zn-2.5%Mg-1.6%Cu alloy inhibited recrystallisation and grain growth and produced considerable grain refinement. The addition of 0.15% Zr instead of Fe, Cr and Mn produced similar grain refinement.
- (2) The addition of 0.17% Fe, 0.15% Cr and 0.11% Mn to Al-6%Zn-2.5%Mg-1.6%Cu alloy increased the proof strength, tensile strength and ductility of the alloy, but reduced the fracture toughness.
- (3) The addition of 0.15% Zr to Al-6.0%Zn-2.5%Mg-1.6%Cu alloy had little effect on proof strength, tensile strength and fracture toughness, but increased tensile ductility and hot formability.
- (4) The application of a special processing treatment to the Al-6%Zn-2.5%Mg-1.6%Cu alloy inhibited recrystallisation and grain growth and increased resistance to stress corrosion crack growth.
- (5) In general, for a given alloy subjected to different processing treatments, the resistance to stress corrosion crack growth increased as the extent of recrystallisation decreased.

(6) For the three alloys hot worked at 400°C or 450°C, resistance to stress corrosion crack growth was greatest for the alloy containing 0.17% Fe, 0.15% Cr and 0.11% Mn and least for the quaternary Al-Zn-Mg-Cu alloy.

(7) The stress corrosion resistance of the alloy containing 0.17% Fe, 0.15% Cr and 0.11% Mn was significantly higher than for the alloy containing 0.15% Zr, for all processing treatments.

Table 1

CHEMICAL COMPOSITIONS OF THE ALLOYS WT%

Alloy		Zn	Mg	Cu	Fe	Mn	Cr	Zr	Ti	Si
1	Top	5.94	2.54	1.49	0.03	nd	nd	nd	nd	nd
	Bottom	5.94	2.49	1.49	0.03	nd	nd	nd	nd	nd
2	Top	5.57	2.25	1.40	0.03	nd	<0.01	0.16	nd	nd
	Bottom	5.87	2.35	1.54	0.03	nd	<0.01	0.15	nd	nd
3	Top	5.87	2.43	1.43	0.17	0.11	0.15	<0.02	0.06	0.03
	Bottom	6.10	2.44	1.51	0.17	0.11	0.15	<0.02	0.06	0.03

nd - none detected

Table 2

MECHANICAL PROPERTIES OF THE ALLOYS, SOLUTION TREATED
AT 465°C, COLD WATER QUENCHED AND AGED 26 h AT 121°C

Production	Alloy	0.2% PS [†] MPa	TS [†] MPa	Elongation [†] % on 5.6√A	K _{1c} ^{††} Mpa m ^{1/2}
Conventional production - hot working at 450°C	1	463 } 466 469 }	531 } 534 537 }	7.5 } 8 7.5 }	26 } 28 30 }
	2	453 } 463 472 }	523 } 529 534 }	16.0 } 16 16.5 }	25 } 27 29 }
	3	499 } 485 472 }	573 } 550 527 }	13.0 } 10 7.0 }	24 } 22 20 }
Special production - hot working at 300°C	1	466 } 470 474 }	537 } 534 531 }	5.0 } 4 3.5 }	29
	2	491 } 478 466 }	551 } 544 536 }	13.0 } 14 15.0 }	27 } 28 29 }
	3	491 } 493 494 }	567 } 569 570 }	13.5 } 13 13.0 }	26 } 24 22 } 24 }
Special production - hot working at 250°C	1	457 } 448 438 }	525 } 512 499 }	5.5 } 5 4.0 }	24
	2	476 } 483 489 }	547 } 553 559 }	14.0 } 15 16.5 }	28 } 28 27 }
	3	497 } 494 491 }	579 } 574 568 }	13.0 } 12 10.5 }	24

† Long transverse orientation

†† Short transverse - longitudinal orientation

Table 3

C-RING STRESS CORROSION TEST RESULTS FOR ALLOYS 1, 2 AND 3,
SOLUTION TREATED AT 465°C, COLD WATER QUENCHED AND AGED 26 h AT 121°C
TIME TO FAILURE OR TIME OF TEST IN DAYS AGAINST STRESS IN MPa

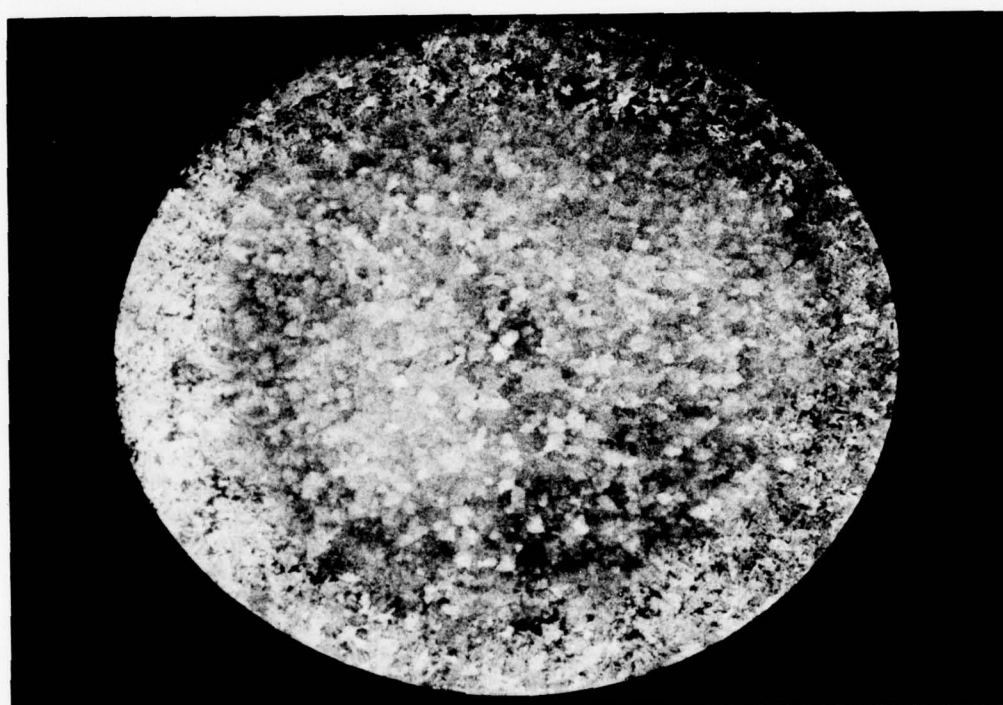
Alloy	Hot worked at	Stress MPa					
		50	100	150	200	250	300
1	400°C	31 ub	31 ub	31 ub	30 ub	30 ub	30 f
		31 ub	31 ub	31 ub	30 ub	30 ub	30 ub
	300°C	31 ub	31 ub	31 ub	31 ub	31 ub	-
		31 ub	31 ub	31 ub	31 ub	31 ub	-
	250°C	31 ub	31 ub	31 ub	31 ub	31 ub	-
		31 ub	31 ub	31 ub	31 ub	31 ub	-
2	450°C	31 ub	31 ub	31 ub	31 ub	31 ub	31 f
		31 ub	31 ub	31 ub	31 ub	31 ub	
	300°C	32 ub	32 ub	32 ub	32 ub	14 f	
		32 ub	32 ub	32 ub	-	30 f	
	250°C	32 ub	32 ub	32 ub	32 ub	32 ub	
		32 ub	32 ub	32 ub	32 ub	32 ub	
3	450°C	32 ub	32 ub	30 ub	30 ub	-	30 ub
		32 ub	32 ub				
	300°C	30 ub	30 ub	30 ub	30 ub	30 ub	30 f
		30 ub	30 ub	30 ub	30 ub	30 ub	30 f
	250°C	30 ub	30 ub	30 ub	30 ub	30 ub	30 ub
		30 ub	30 ub	30 ub	30 ub	30 ub	30 ub

ub - unbroken on completion of test, this fact being confirmed by microsection

REFERENCES

- | <u>No.</u> | <u>Author</u> | <u>Title, etc</u> |
|------------|--|--|
| 1 | M.K.B. Day
A.J. Cornish
T.P. Dent | The relationship between structure and stress corrosion life in an Al-Zn-Mg alloy.
Met. Sci. Jnl., <u>3</u> , p 175 (1969) |
| 2 | R.W. Elkington | The effect of sub-structure on stress corrosion cracking of commercial Al-Zn-Mg alloys.
JIM, <u>90</u> , p 267 (1961-62) |
| 3 | M. Van Lancker | Metallurgy of Al alloys.
Chapman and Hall, London (1967) |
| 4 | J.C. Blade
A.J. Bryant
A.T. Thomas | Alloy composition and microstructure control in relation to mechanical working for Al alloys.
Metals Technology, <u>3</u> , 8, p 380 (1976) |
| 5 | R. Grimes | Grain control in Al.
Met. Sci. Jnl., <u>8</u> , p 176 (1974) |
| 6 | Committee B3 | Stress corrosion testing methods.
ASTM STP 425 (1967) |
| 7 | M.V. Hyatt | The use of pre-cracked specimens in stress corrosion testing on high strength Al alloys.
Corrosion, <u>26</u> , 11, p 487 (1970) |
| 8 | C.J. Peel
P.J.E. Forsyth | The effect of composition changes on the fracture toughness of an Al-Zn-Mg-Cu forging alloy.
Met. Sci. Jnl., <u>7</u> , p 121 (1973) |
| 9 | C.J. Peel
P.J.E. Forsyth | Fracture toughness of Al-Zn-Mg-Cu-Mn alloys to DTD 5024.
RAE Technical Report 72173 (1972) |
| 10 | C.J. Peel
P. Poole | Stress corrosion resistance of high strength Al-Zn-Mg-Cu alloys - solute depletion.
RAE Technical Report 77148 (1977) |
| 11 | B.R.W. Hinton | The effects of additions of Cr, Ag and Mn on the stress corrosion behaviour of an Al-Zn-Mg-Cu alloy.
ARL/Mat 111 (1975) |

Fig 1



x 3/4

Fig 1 Etched macrosection of the bottom of the cast ingot of Alloy 1,
Al-Zn-Mg-Cu

Figs 2&3

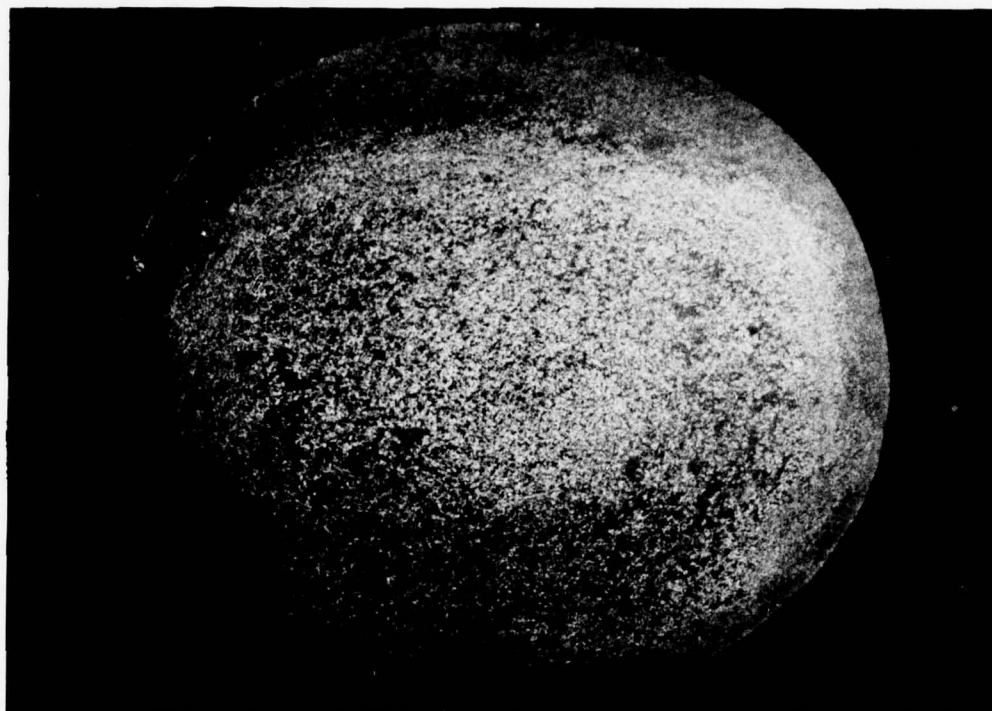


Fig 2 Etched macrosection of the bottom of the cast ingot of Alloy 2,
Al-Zn-Mg-Cu-Zr

$\times \frac{3}{4}$

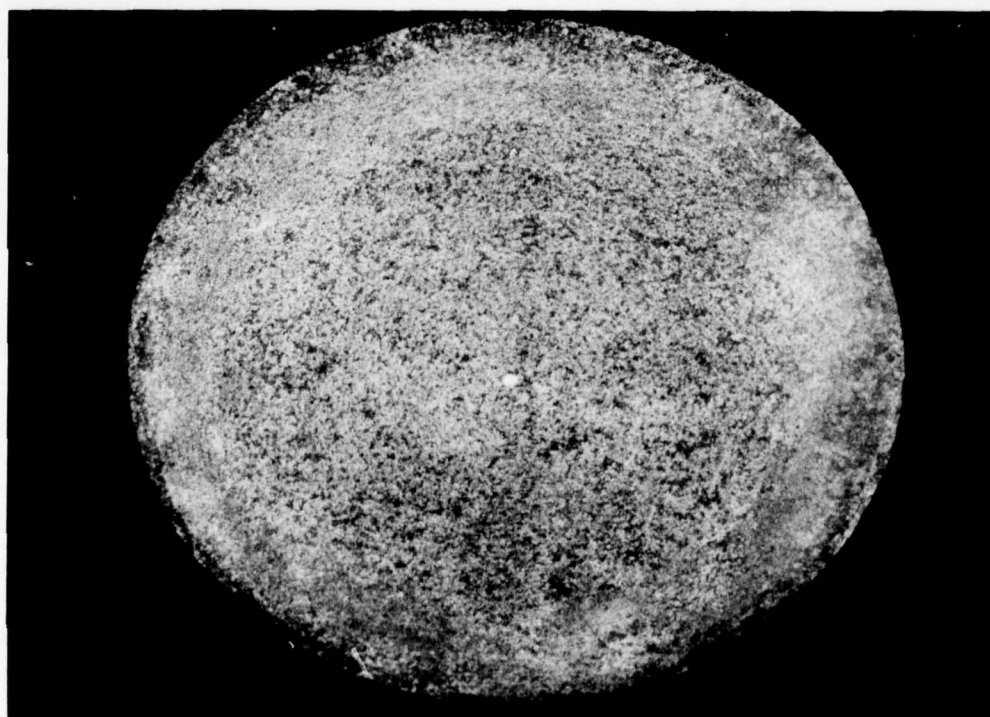
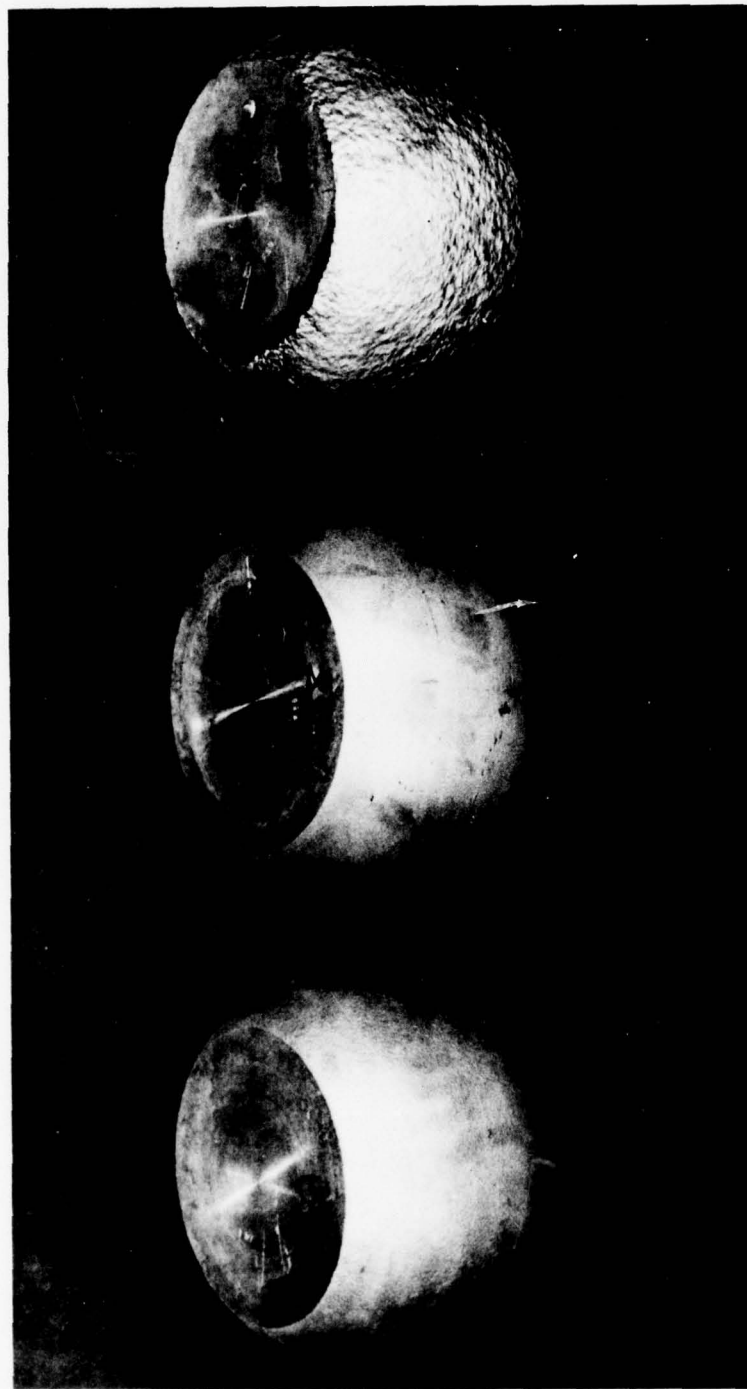


Fig 3 Etched macrosection of the bottom of the cast ingot of Alloy 3,
Al-Zn-Mg-Cu-Fe-Cr-Mn

$\times \frac{3}{4}$



Alloy 3, Al-Zn-Mg-Cu-Fe-Cr-Mn Alloy 2, Al-Zn-Mg-Cu-Zr Alloy 1, Al-Zn-Mg-Cu $\times \frac{1}{4}$

Fig 4 The three alloy billets after the first longitudinal pressing. Note the effects of grain refiners

Fig 4

Fig 5

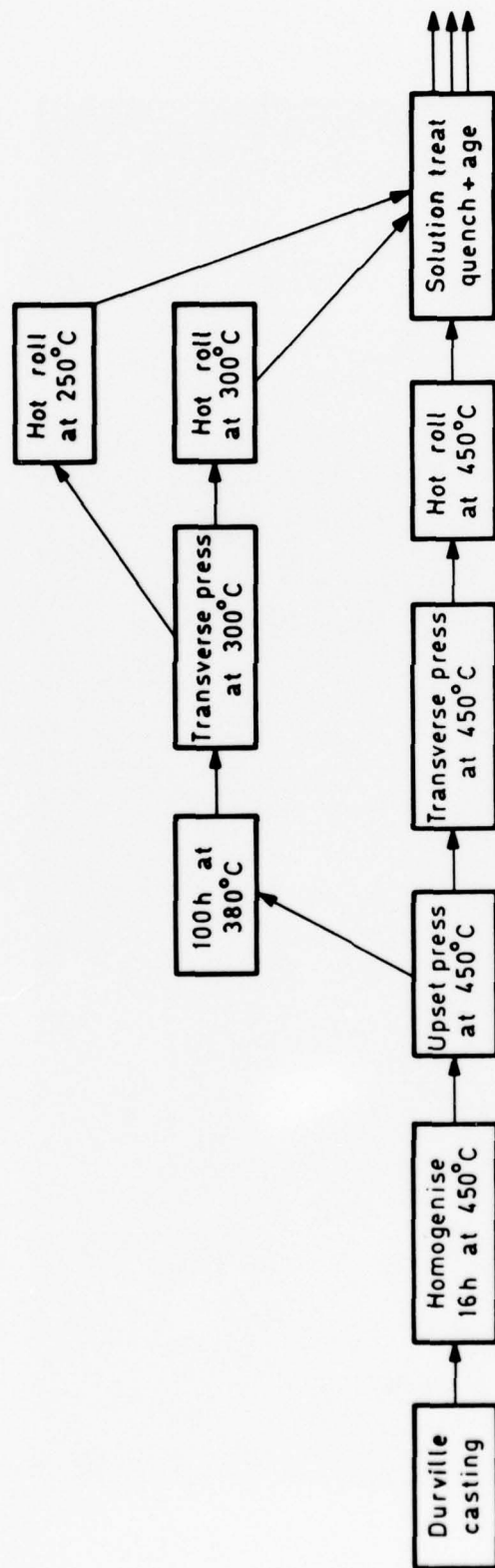
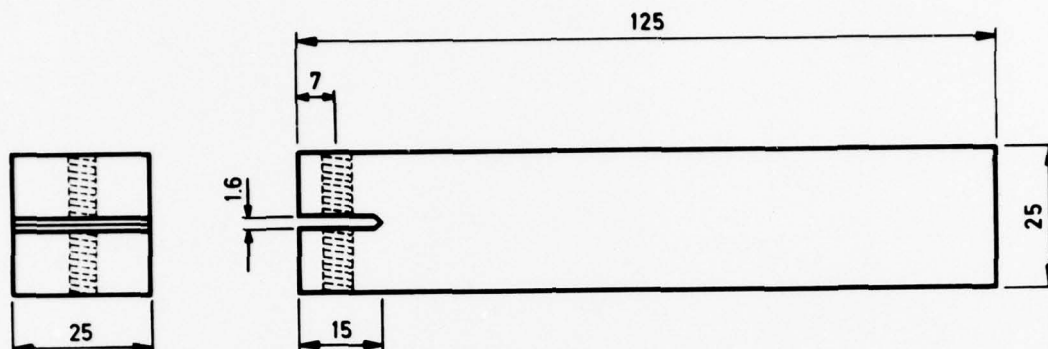


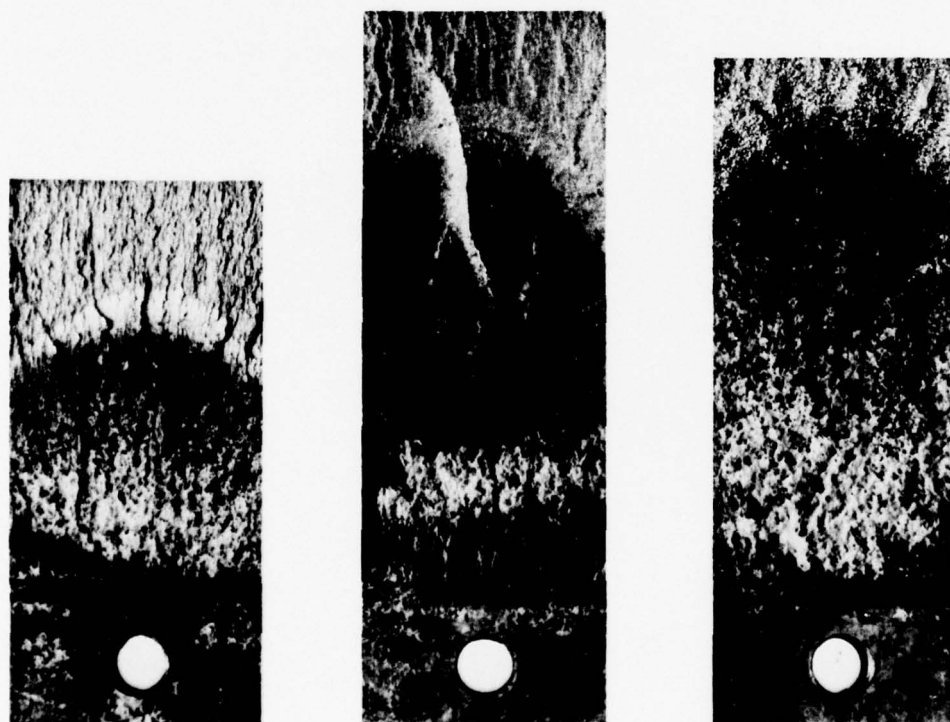
Fig 5 Fabrication processes for the three alloys.
NB. For alloy 1, pressing and rolling was at 400°C not 450°C

Figs 6&7



Dimensions in mm

Fig 6 The dimensions of the double cantilever beam test pieces



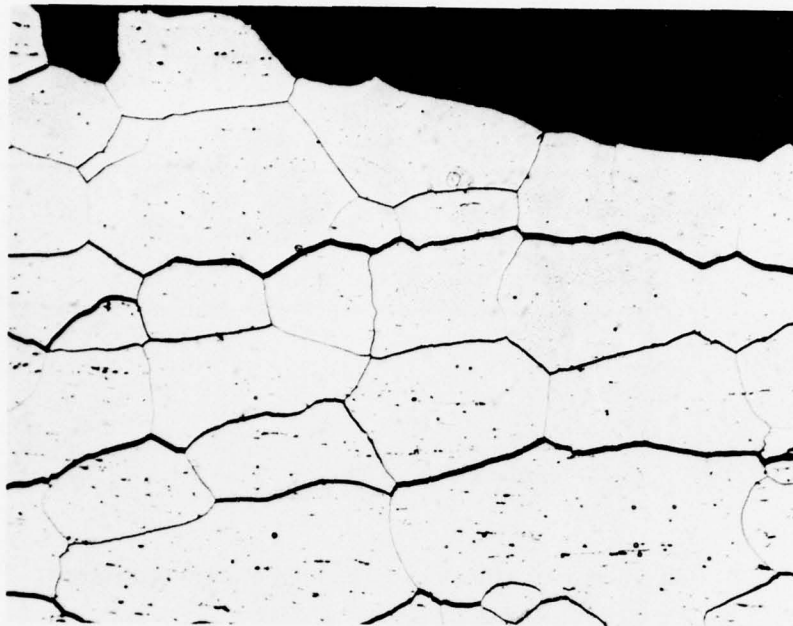
Alloy 3 - 450

Alloy 2 - 450

Alloy 1 - 400 x1½

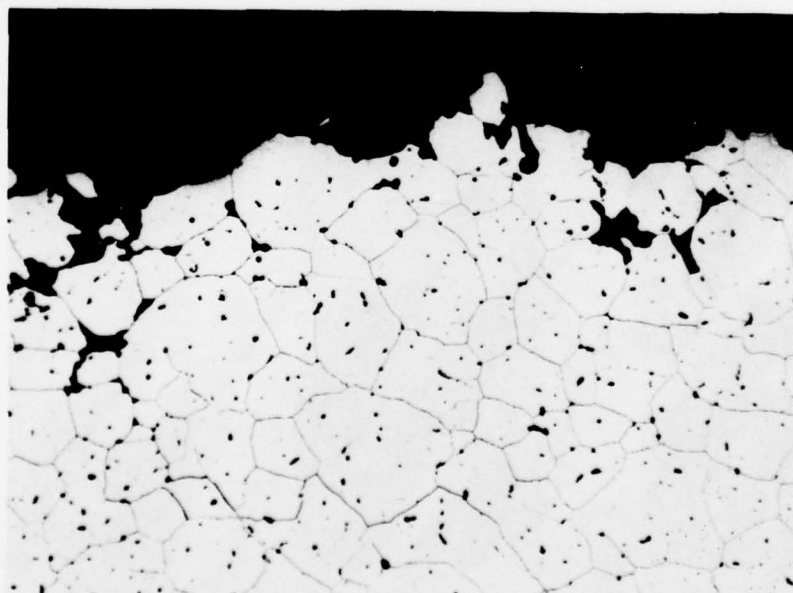
Fig 7 The fracture surfaces of DCB test pieces broken open after testing

Figs 8&9



x100

Fig 8 Microsection of a DCB test piece of Alloy 1, worked at 400°C, etched in Wasserman's reagent



x100

Fig 9 Microsection of a DCB test piece of Alloy 1, given special processing and worked at 300°C, etched in Wasserman's reagent

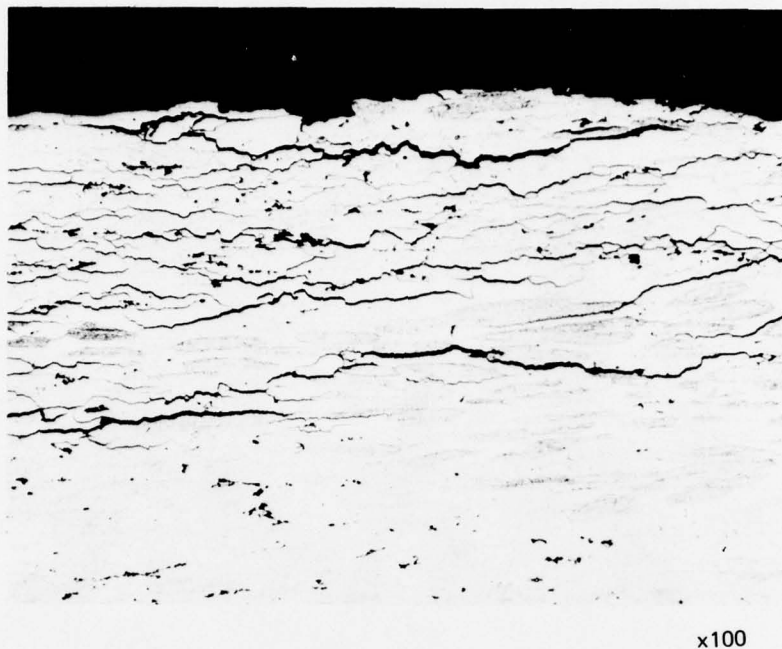


Fig 10 Microsection of a DCB test piece of Alloy 1, given special processing and worked at 250°C, etched in Wasserman's reagent

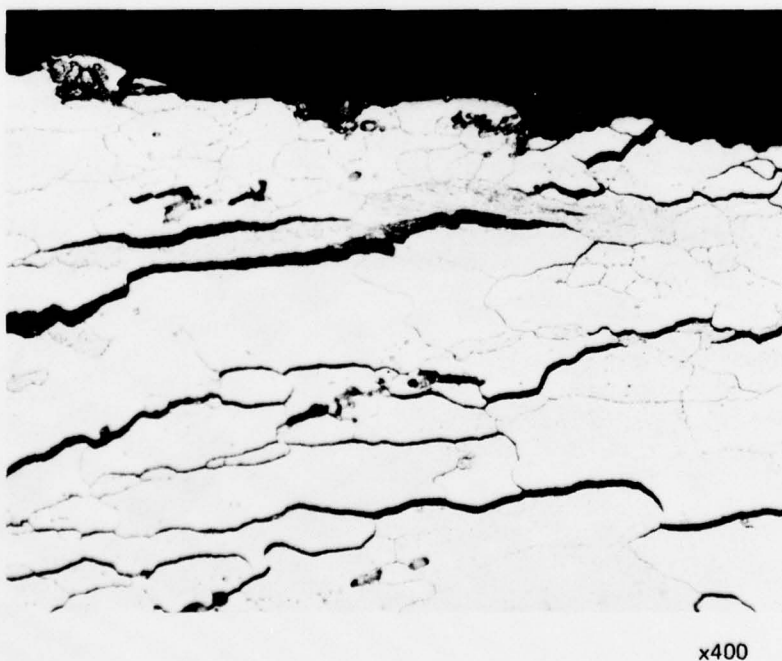


Fig 11 Microsection of a DCB test piece of Alloy 1, given special processing and worked at 250°C, etched in Wasserman's reagent

Figs 12&13

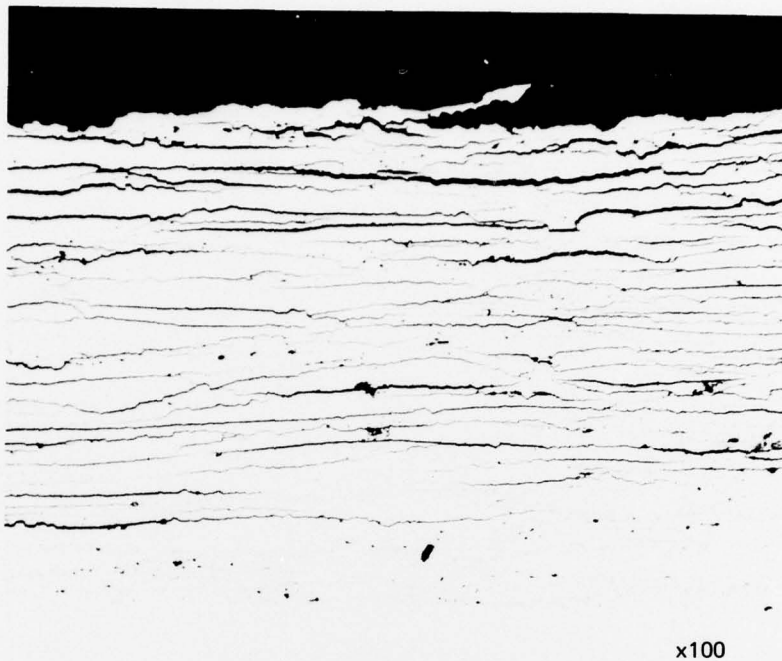


Fig 12 Microsection of a DCB test piece of Alloy 2, worked at 450°C, etched in Wasserman's reagent

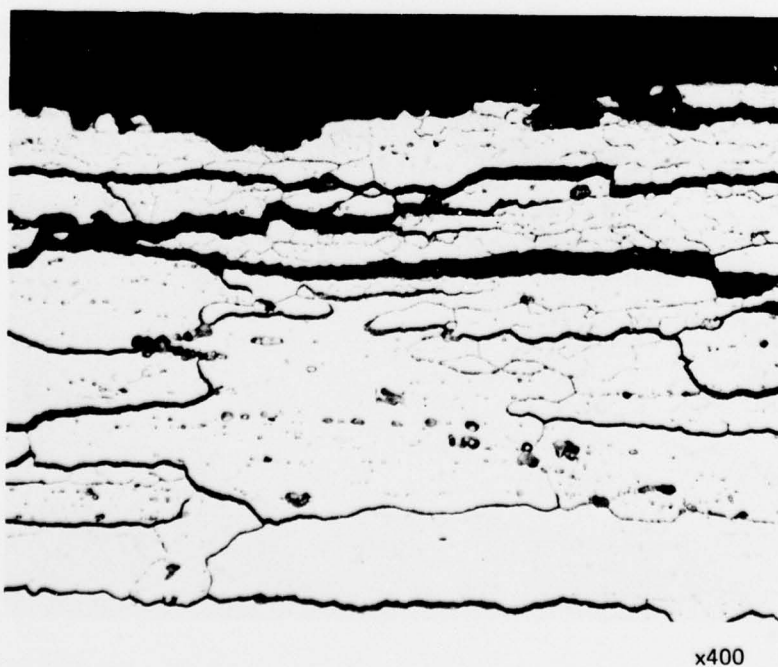
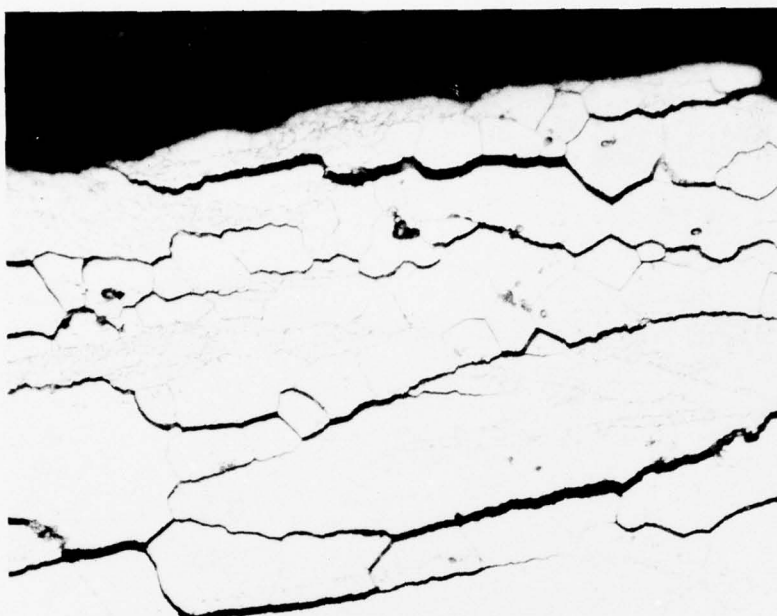
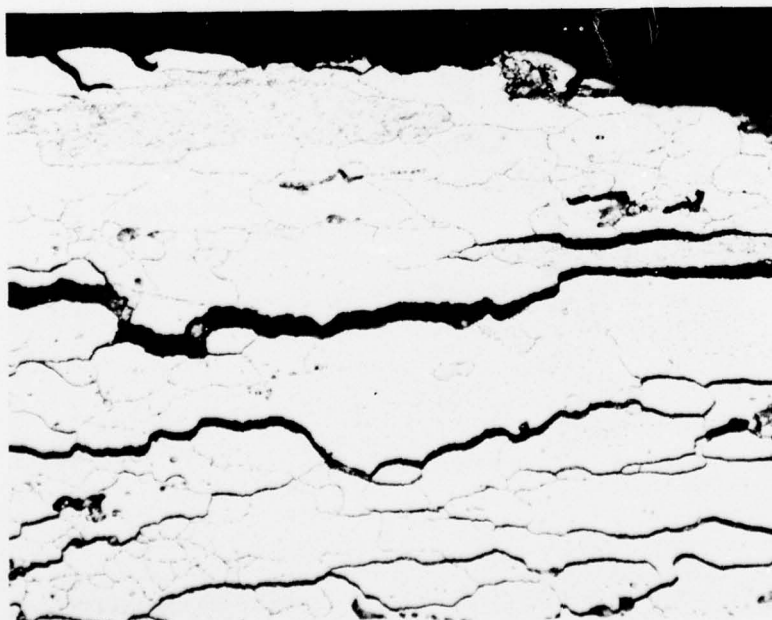


Fig 13 Microsection of a DCB test piece of Alloy 2, worked at 450°C, etched in Wasserman's reagent



x400

Fig 14 Microsection of a DCB test piece of Alloy 2, given special processing and worked at 300°C, etched in Wasserman's reagent



x400

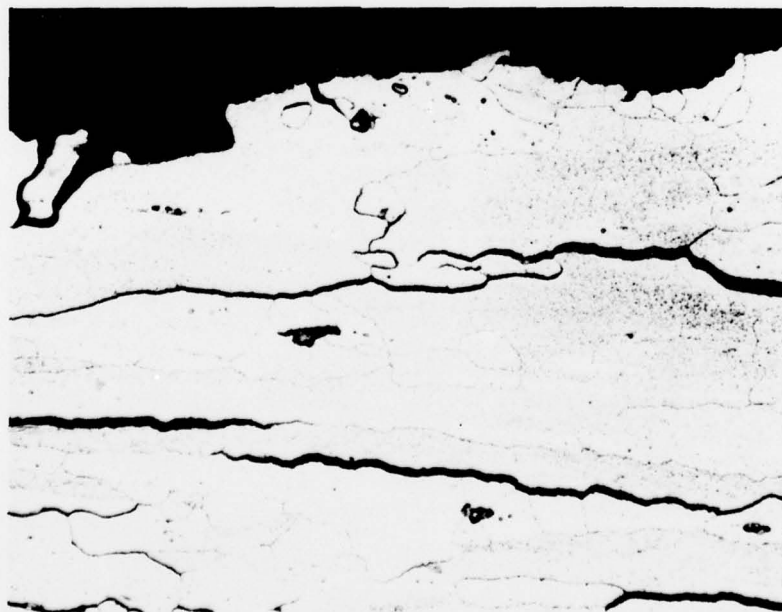
Fig 15 Microsection of a DCB test piece of Alloy 2, given special processing and worked at 250°C, etched in Wasserman's reagent

Figs 16&17



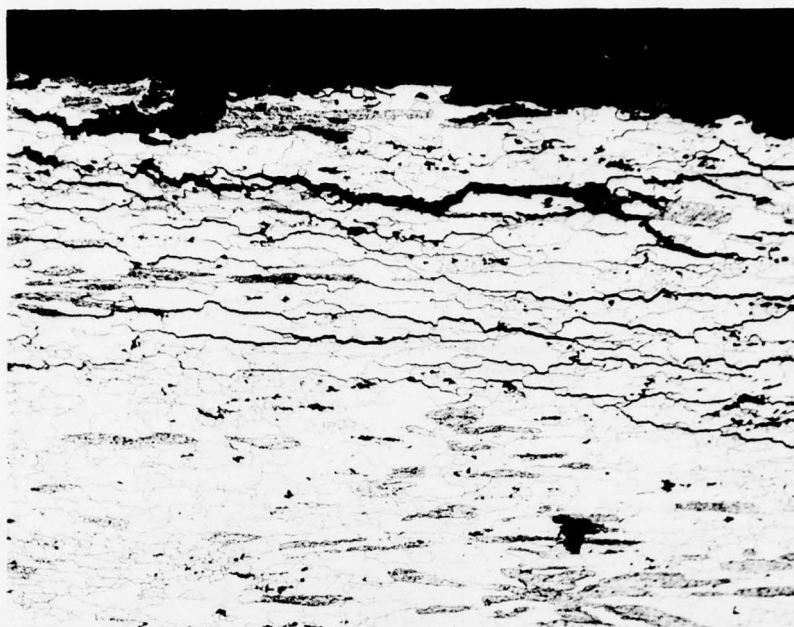
x400

Fig 16 Microsection of a DCB test piece of Alloy 3, worked at 450°C, etched in Wasserman's reagent



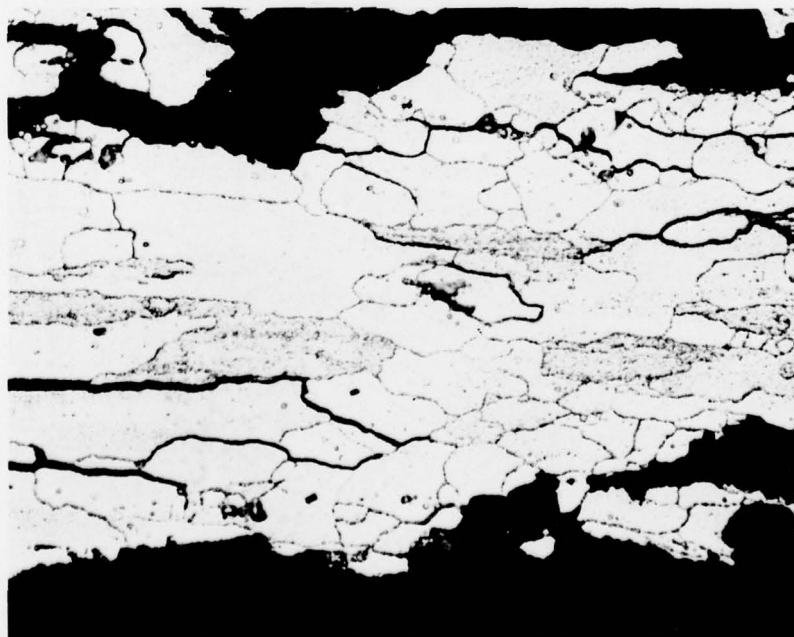
x400

Fig 17 Microsection of a DCB test piece of Alloy 3, given special processing and worked at 300°C, etched in Wasserman's reagent



x100

Fig 18 Microsection of a DCB test piece of Alloy 3, given special processing and worked at 250°C, etched in Wasserman's reagent



x400

Fig 19 Microsection of a DCB test piece of Alloy 3, given special processing and worked at 250°C, etched in Wasserman's reagent

Fig 20

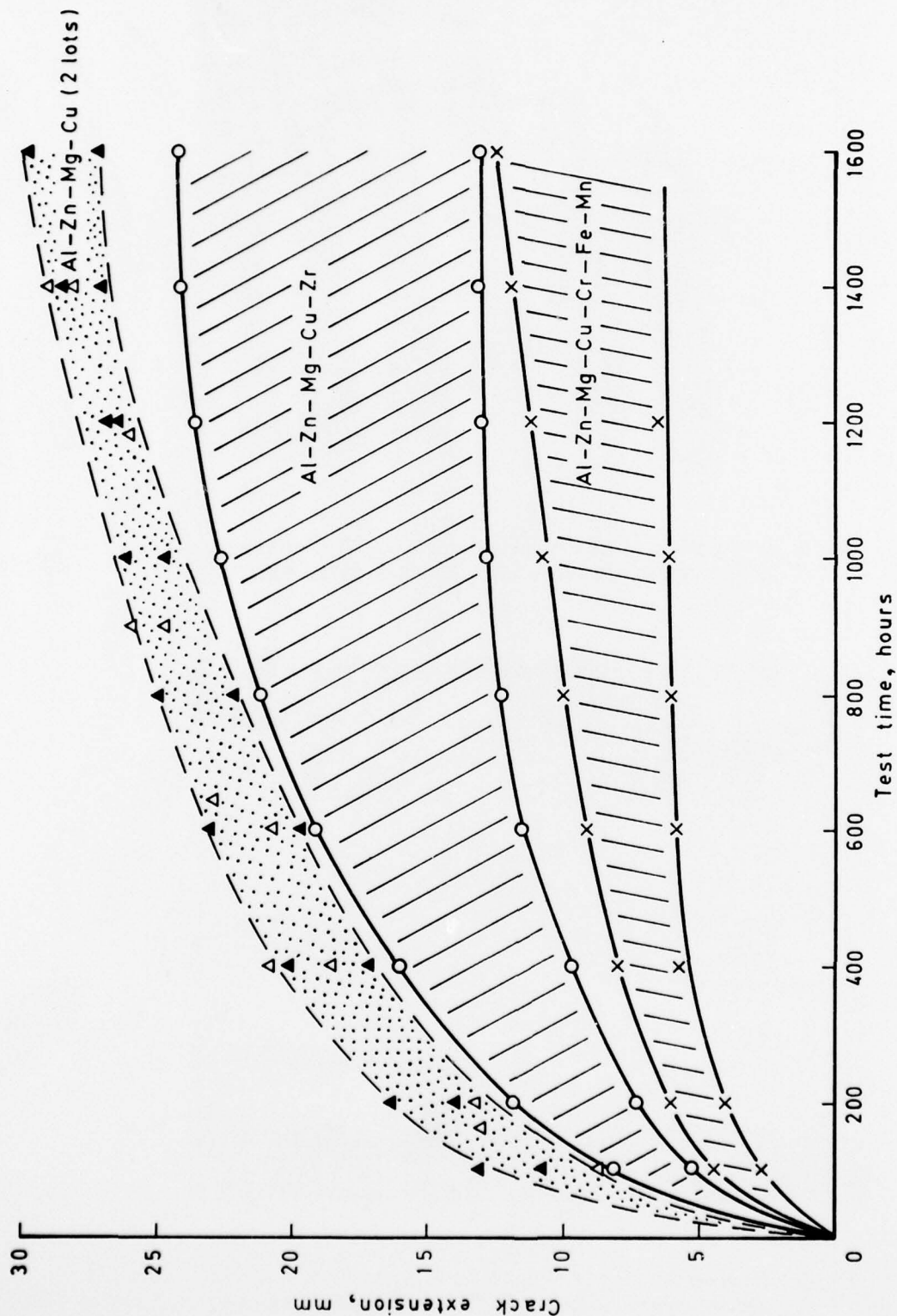


Fig 20 Crack extension as a function of test time for DCB stress corrosion tests of the three alloys given a conventional working process at 450°C

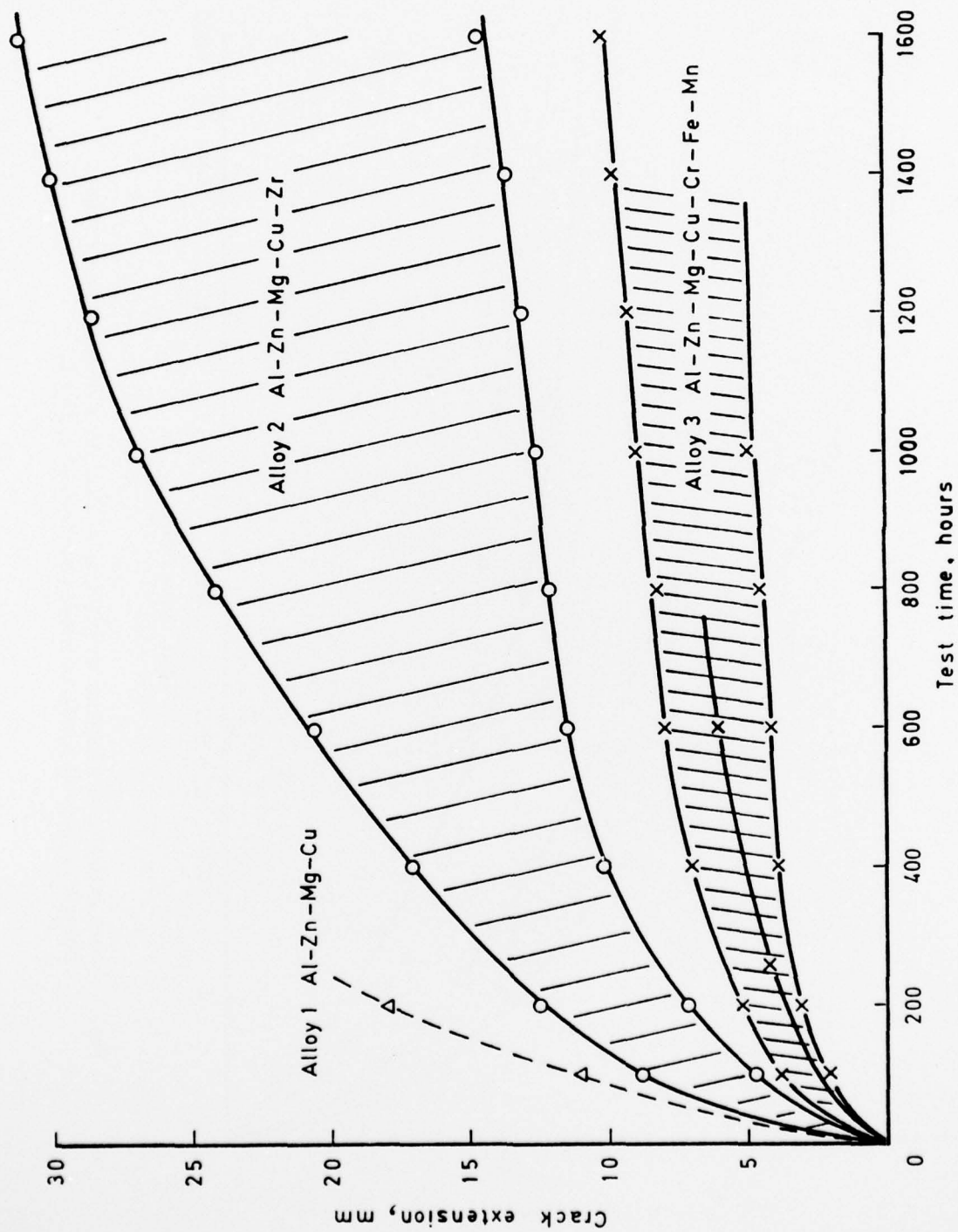


Fig 21 Crack extension as a function of test time for DCB stress corrosion tests of the three alloys given the special processing and worked at 300°C

Fig 22

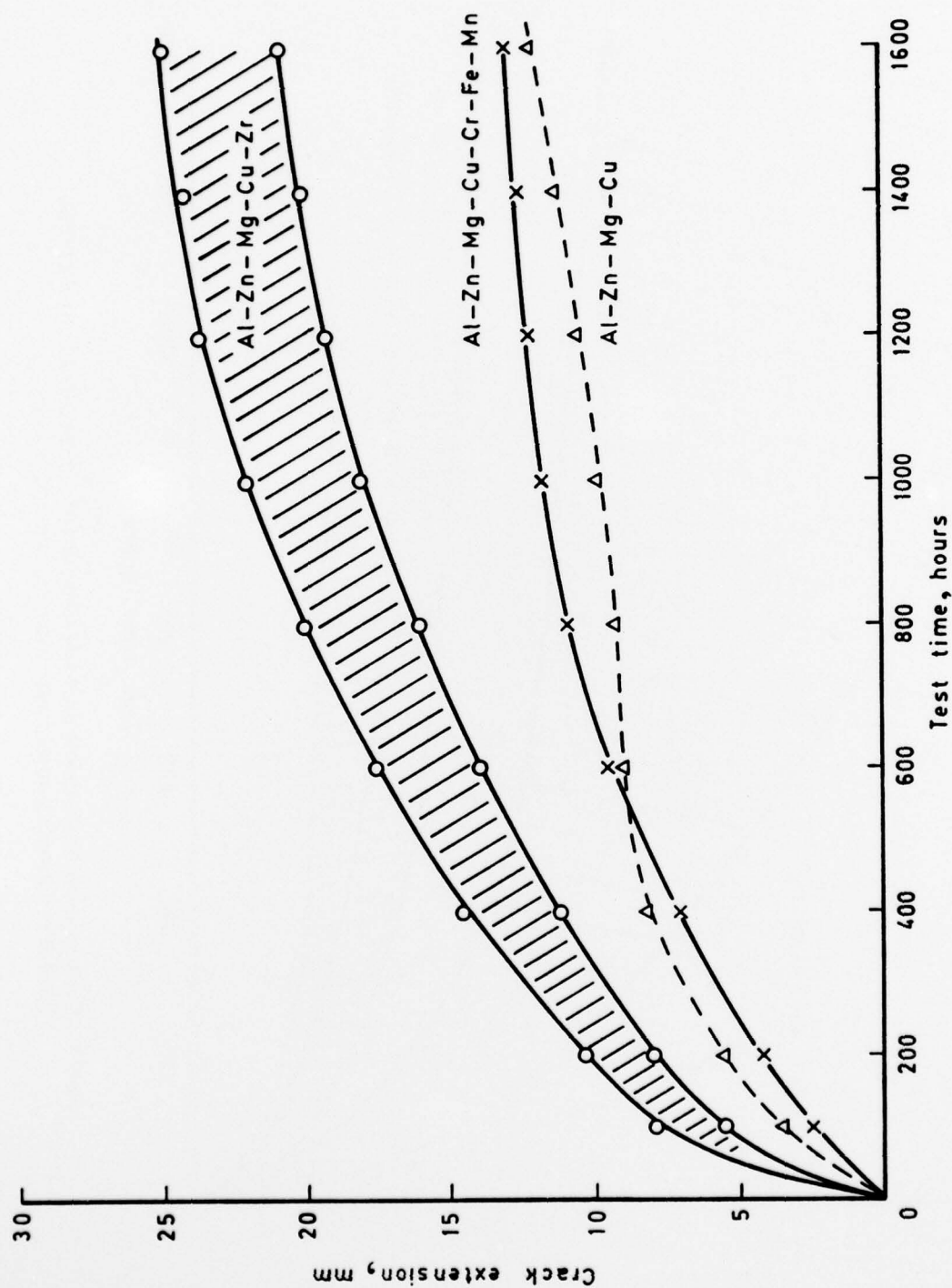


Fig 22 Crack extension as a function of test time for DCB stress corrosion tests of the three alloys given the special processing and worked at 250°C

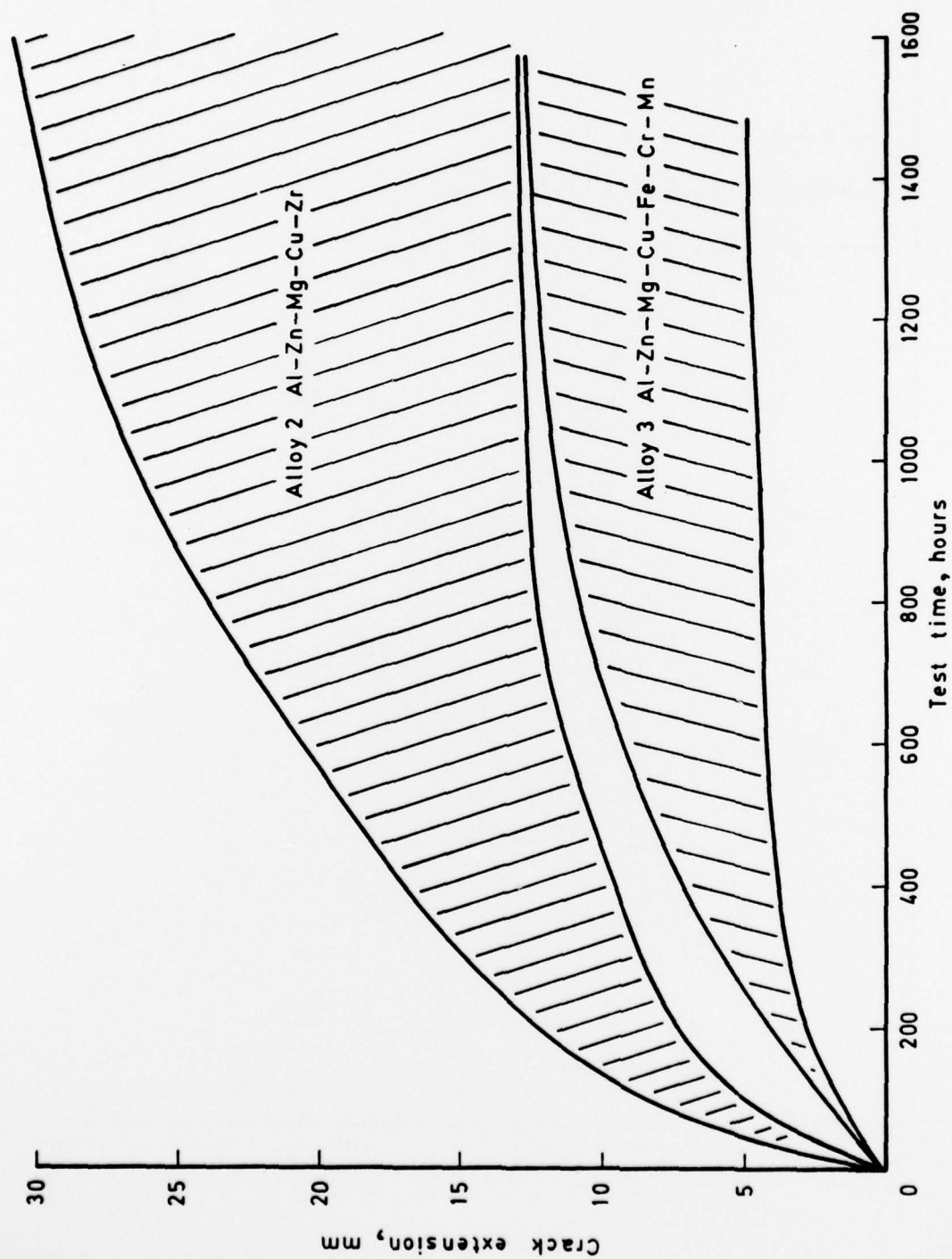


Fig 23 Crack extension as a function of test time for all DCB stress corrosion tests of alloys 2 and 3

Fig 24

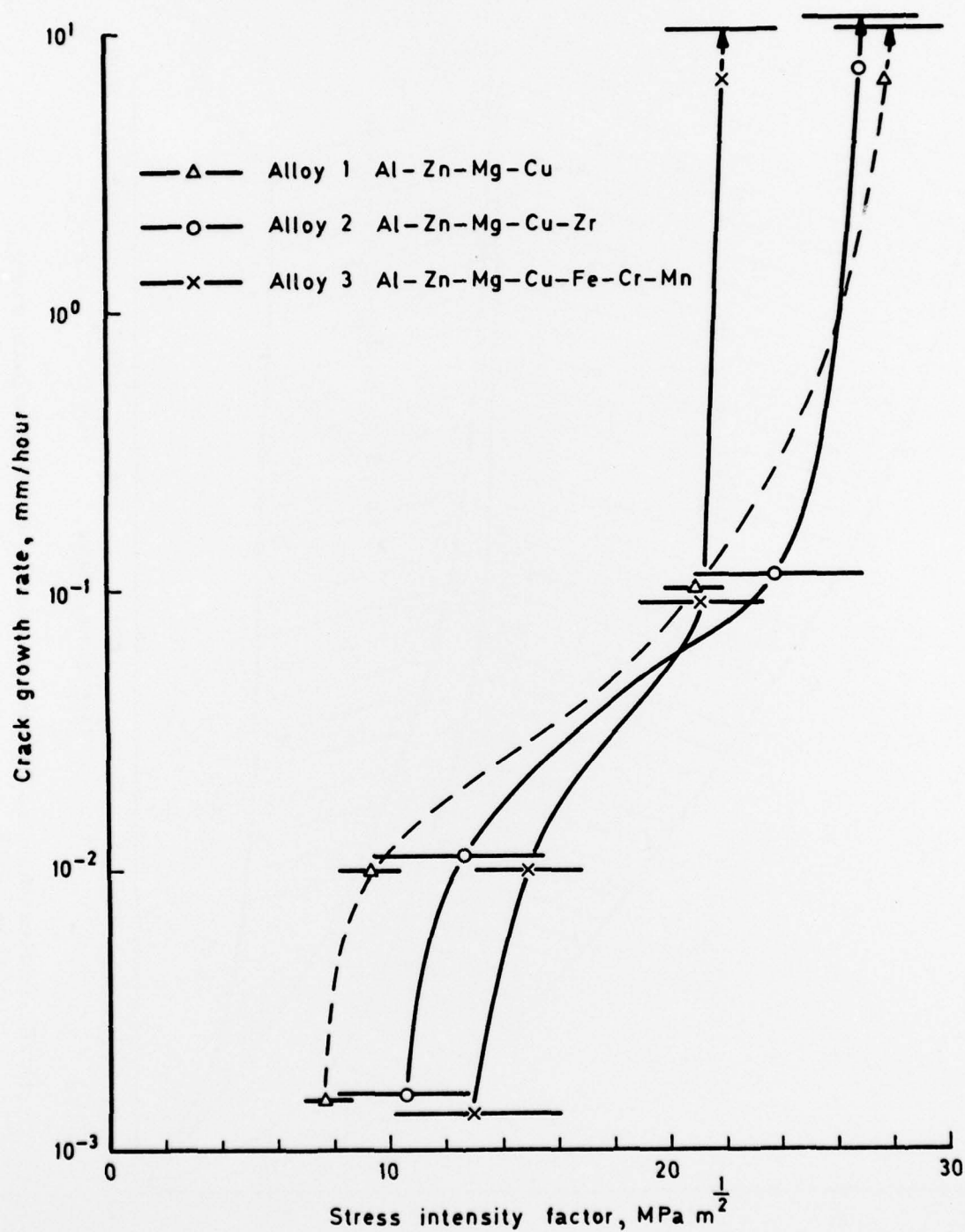


Fig 24 Stress corrosion crack growth rates, in the three alloys given a conventional working treatment at 450°C, plotted as a function of stress intensity factor

Fig 25

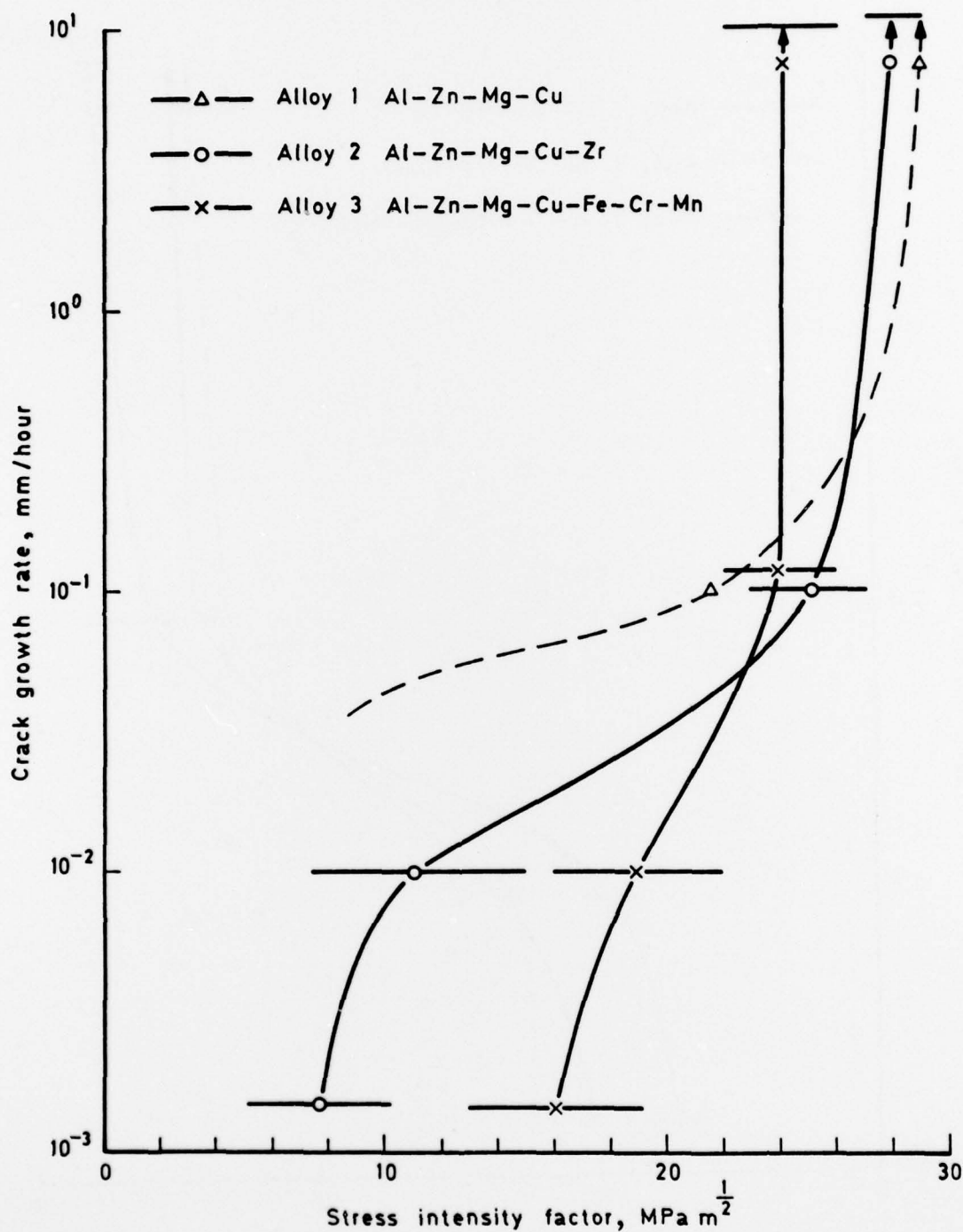


Fig 25 Stress corrosion crack growth rates, in the three alloys given the special processing and worked at 300°C, plotted as a function of stress intensity factor

Fig 26

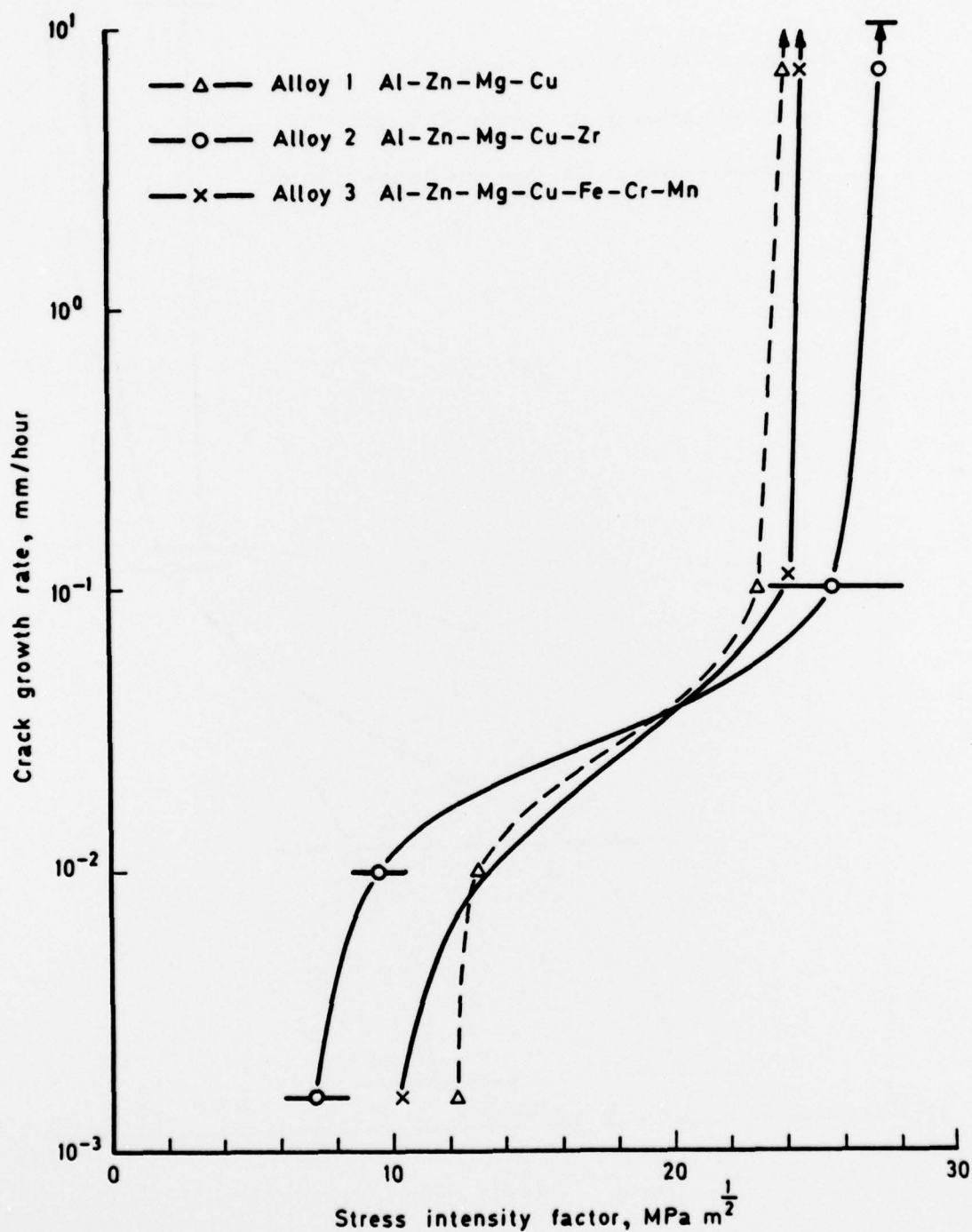


Fig 26 Stress corrosion crack growth rates, in the three alloys given the special processing and worked at 250°C , plotted as a function of stress intensity factor

REPORT DOCUMENTATION PAGE

Overall security classification of this page

UNCLASSIFIED

As far as possible this page should contain only unclassified information. If it is necessary to enter classified information, the box above must be marked to indicate the classification, e.g. Restricted, Confidential or Secret.

1. DRIC Reference (to be added by DRIC)	2. Originator's Reference RAE TR 78034	3. Agency Reference N/A	4. Report Security Classification/Marking UNCLASSIFIED		
5. DRIC Code for Originator 850100		6. Originator (Corporate Author) Name and Location Royal Aircraft Establishment, Farnborough, Hants, UK			
5a. Sponsoring Agency's Code N/A		6a. Sponsoring Agency (Contract Authority) Name and Location N/A			
7. Title The effect of grain structure on the stress corrosion resistance of Al-Zn-Mg-Cu alloys					
7a. (For Translations) Title in Foreign Language					
7b. (For Conference Papers) Title, Place and Date of Conference					
8. Author 1. Surname, Initials Peel, C.J.	9a. Author 2 Poole, P.	9b. Authors 3, 4		10. Date April 1978	Pages 34
11. Contract Number N/A		12. Period N/A		13. Project 14. Other Reference Nos. Mat 344	
15. Distribution statement (a) Controlled by - RAE TR 78034 (b) Special limitations (if any) - None					
16. Descriptors (Keywords) (Descriptors marked * are selected from TEST) Aluminium alloys. Grain structure. Stress corrosion cracking.					
17. Abstract Three alloys, Al-6%Zn-2.5%Mg-1.5%Cu, Al-6%Zn-2.5%Mg-1.5%Cu-0.15%Zr and Al-6%Zn-2.5%Mg-1.5%Cu-0.17%Fe-0.15%Cr-0.11%Mn were produced as 37mm plate in the T6 condition. The stress corrosion resistance, fracture toughness and tensile properties of the alloys were determined to identify the effects of the grain refining elements, Zr, Cr, Fe and Mn on these properties. A special processing treatment, involving extensive precipitation and warm working, was also applied to pieces of plate to produce an extensively recrystallised structure, with a small grain size, for comparison with the coarser structures of the conventionally worked alloys. The results indicated that the alloy containing Fe, Cr and Mn had the highest stress corrosion resistance and strength but the lowest fracture toughness. The addition of 0.15% Zr to the quaternary alloy slightly improved the tensile strength and stress corrosion resistance but had no effect on fracture toughness. However this addition of Zr markedly improved the hot workability of the alloy and increased its tensile ductility. Special processing and working at 250°C was beneficial to the stress corrosion resistance of the quaternary alloy but detrimental to that of the other two alloys containing Zr or Fe, Cr and Mn. It was concluded that, in these Al-Zn-Mg-Cu alloys, a recrystallised grain structure has a low stress corrosion resistance and that inhibiting recrystallisation increases stress corrosion resistance.					

5910